Yoon, J.-S., Zang, A., Stephansson, O., Hofmann, H., Zimmermann, G. (2017): Discrete Element Modelling of Hydraulic Fracture Propagation and Dynamic Interaction with Natural Fractures in Hard Rock. - *Procedia Engineering*, *191*, pp. 1023—1031.

DOI: http://doi.org/10.1016/j.proeng.2017.05.275

Available online at www.sciencedirect.com

ScienceDirect

Procedia Engineering 191 (2017) 1023 – 1031

Procedia Engineering

www.elsevier.com/locate/procedia

Symposium of the International Society for Rock Mechanics

Discrete Element Modelling of Hydraulic Fracture Propagation and Dynamic Interaction with Natural Fractures in Hard Rock

Jeoung Seok Yoon[a]*, Arno Zang[a], Ove Stephansson[a],

Hannes Hofmann[b], Günter Zimmermann[b]

[a]*Section 2.6 Seismic Hazard and Stress Field, Helmholtz Centre Potsdam GFZ German Research Centre for Geosciences, Telegrafenberg, Potsdam D14473, Germany*

[b]*Section 6.2 Geothermal Energy Systems, Helmholtz Centre Potsdam GFZ German Research Centre for Geosciences, Telegrafenberg, Potsdam D14473, Germany*

Abstract

In this study, we used the Particle Flow Code 2D (PFC2D) to simulate interaction of hydraulic fractures and natural fractures in low permeable hard rock. Natural fractures are simulated using the smooth joint model of PFC2D. We modified our fluid flow algorithm to model larger fracture permeability, and we investigated interactions of hydraulic fractures and natural fractures by varying the angle of approach and viscosity of the fracturing fluid. We also investigated seismic events evolving in a complex fracture network. The results demonstrate that our modelling tool is able to capture all possible interactions of hydraulic and natural fractures: Arrest, Crossing, Slippage of hydraulic fracture, Dilation of natural fracture, Closing/Opening of natural fracture. With low angle of approach, the hydraulic fracture coalesces with the natural fractures and results in hydro-shearing and propagation of hydro-wing fractures at the tips that are mostly Mode I type. We tested the model containing multiple natural fractures with varied fluid viscosity. Hydraulic fracture generated by high viscosity fluid tends to be localized, linear and less influenced by the natural fractures. In the complex network of natural fractures, fluid columns built along the fracture network increase the local state of stress by stress shadowing. Hydro-shearing of the natural fractures that were under increased stress state can be explained as the main mechanism responsible for occurrence of larger magnitude microseismic events.

Peer-review under responsibility of the organizing committee of EUROCK 2017

Keywords: Hydraulic fracturing; Fracture interaction; Fracture permeability; Large magnitude microseismicity; Stress Shadowing; EGS

* Corresponding author. Tel.: +49-331-288-1716; fax: +49-331-288-1127.
E-mail address: jsyoon@gfz-potsdam.de

Peer-review under responsibility of the organizing committee of EUROCK 2017
doi:10.1016/j.proeng.2017.05.275

1. Introduction

Geothermal energy stored in the deep subsurface especially in low permeable and hard crystalline rock mass can be accessed by enlarging the surface area where the injected fluid makes contacts to rock mass containing geothermal heat and by increasing the flow rates of the injected fluid through natural pre-existing fracture. These two concepts contribute in the oil and gas industry and enhanced geothermal system to improve the productivity of the hydrocarbon and the geothermal heat energy, respectively.

One of the key factors in successful creation of an efficient subsurface heat exchanger is to predict the propagation of hydraulic fractures (HF) and their interaction with natural pre-existing fractures (NF). There are a number of numerical codes that can simulate interactions of HF and NF, e.g. UDEC [1]. However, not many of these codes are able to simulate the dynamic processes involved in the HF-NF interaction, i.e. evolution of seismicity in HF-NF interactions.

In this paper, we present a series of numerical modellings of HF propagation and their interactions with NF in low permeable and brittle hard rock. We focus on the dynamic mechanisms of HF-NF interaction and see how the seismicity evolves spatially and temporally when HFs and NFs interact.

We use the Particle Flow Code 2D [2] where we implemented fluid flow and seismicity computing algorithms [3]. Compared to several previous modelling studies of ours [3–6], we have further developed the fluid flow algorithm so that the natural pre-existing fractures, that are represented by a collection of smooth joint contacts of PFC2D [7], have a higher permeability compared to those contacts in the intact rock part. This also means that the pre-existing fractures have a certain level of capacity for storing fluid.

2. HF-NF interactions

Chuprakov et al. [8] summarized possible HF-NF interactions as shown in Fig. 1. A HF is created from the fluid injection borehole and propagates through the intack rock. After making contact with the NF, the HF can either be arrested by the NF (Fig. 1a, Arrest) or continue propagation across the NF (Fig. 1b, Crossing). In case of being arrested due to a shallow angle of approach, the HF may slip (Fig. 1c, HF slippage) and the NF dilates (Fig. 1c, NF dilation). In case of a steep angle of approach where the HF crosses the NF, the NF may either stay closed (Fig. 1d, NF staying closed) or dilate (Fig. 1e, NF opening). These five possible interaction scenarios are to be tested in this numerical modelling study and we try to seek if there is another unknown mechanism, in particular in terms of dynamics, involved in the HF-NF interactions.

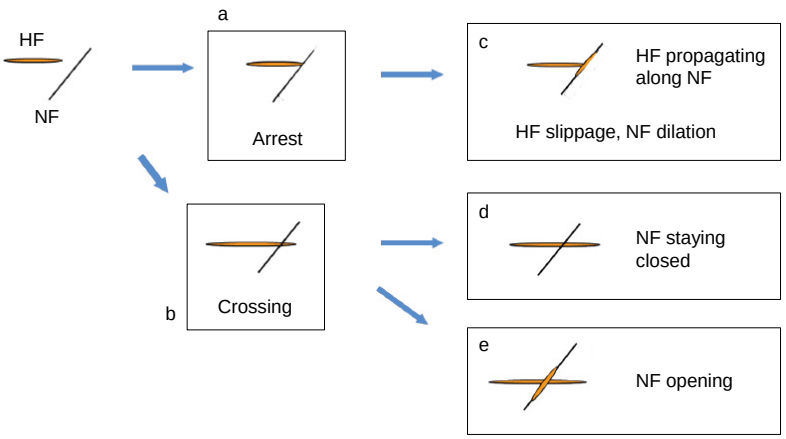

Fig. 1. Schematic diagram of possible hydraulic fracture (HF) and natural fracture (NF) interaction scenarios (modified from [8]).

3. Model description

We set up four models for testing the HF-NF interactions. The models are 4 m x 4 m in size and contain an injection boreholeat the centre with a diameter of 0.05 m. The first two models (Fig. 2a and 2b) contain two fractures with half-lengths of 0.5 m and 30° (Fig. 2a) and 60° (Fig. 2b) inclination with respect to the maximum principal stress direction (horizontal 15 MPa). Fluid with viscosity of 1e-3 Pa·s is injected at the model centre with a rate of 1e-3 m^3/s. The first two models are intended to show and compare the evolution of seismicity and fracture interaction depending on the angle of approach of the HF to the NF. The third model (Fig. 2c) contains two sets of fractures with the same length and 60° inclination on each side of the injection well. The fracture centres are placed offset from the borehole in order to simulate how the HF propagating from the borehole interacts first with the nearest NF and interacts further with the second set of NFs. In this model, the fluid viscosity is varied in two levels: 1e-3 Pa·s and 100e-3 Pa·s, to see the influence of the fluid viscosity on the fracture propagation pattern. The fourth model (Fig. 2d) contains a complex network of fracture sets. The key question studied in this model is how the fracture network behaves and how the seismicity cloud evolves with migration of the fluid.

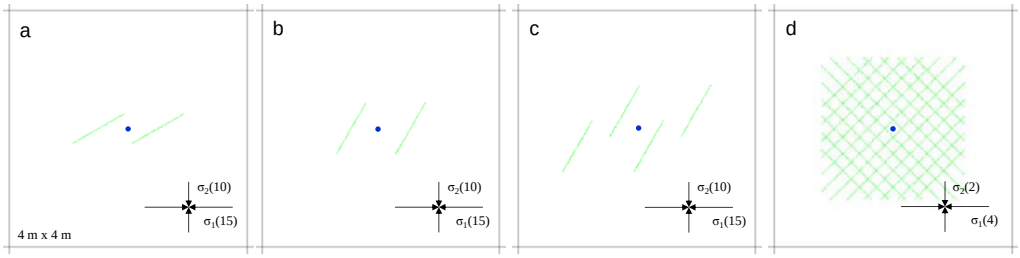

Fig. 2. PFC2D models for testing HF-NF interaction. The models are 4 m x 4 m in size (a and b) two-fracture model with different angles of inclination (30° and 60°) with respect to σ_1; (c) four-fracture model inclined 60° with respect to σ_1; and (d) complex network of fracture sets. Blue dots are the location of fluid injection. The numbers of the arrows are the principal stresses applied to the model in unit of MPa.

The rock model is pre-conditioned to have a permeability k of 1e-16 m^2, simulating a low permeable rock block. The rock model is also pre-conditioned in terms of strength and deformation by assigning high tensile strength and cohesion to the particle contacts to represent a hard crystalline rock. The fractures are modelled using the smooth joint contact model of PFC which has been applied in modelling synthetic rock mass [7]. The properties of the fractures are synthetic but set similar to those taken from a crystalline rock mass at Forsmark (Sweden) where the construction of a final repository for spent nuclear fuel is planned [9]. We use the parallel-bond model for the rock matrix and the smooth joint model for the fractures. For the seismicity computation, we assign a high seismic quality factor Q of 200 and S-wave velocity of 3000 m/s to mimic an undisturbed granitic rock block. The seismic quality factor Q is set to 200 to simulate the attenuation characteristics of Lac du Bonnet granite [10].

Table 1. Model parameters.

Property (Unit)	Rock matrix	Fracture
Particle density (kg/m^3)	2630	NA
Young's modulus (GPa)	60	NA
Friction coefficient (-)	0.9	0.6
Tensile strength (MPa)	9	0.1
Cohesion (MPa)	25	0.5
Friction angle (Deg)	53	30
Dilation angle (Deg)	NA	3
Normal stiffness (GPa/m)	NA	600
Shear stiffness (GPa/m)	NA	50
Hydraulic aperture at zero σ_n, e_0 (μm)	2.7	27
Hydraulic aperture at ∞ σ_n, e_∞ (μm)	1	10
Coefficient of decay, α	0.1	0.05

In this study, we have further upgraded the hydro-mechanical coupled fluid flow algorithm by enabling the embedded fractures to behave differently from the rock matrix. This is done by assigning different relations of hydraulic aperture (e) and normal stress (σ_n). Figure 3 shows two curves of hydraulic aperture and normal stress relations applied to the particle contacts in the rock matrix (red) and in the fractures (blue). Hydraulic aperture at a particle contact in the rock matrix part under zero normal stress (e_0) is 3 μm and decreases with increasing normal stress and reaches 1 μm under high normal stress (e_∞). For the fractures, the hydraulic aperture at zero normal stress is 30 μm and reaches 10 μm at high normal stress. Initially, as the model is under stress, the hydraulic apertures both for the rock matrix and the fractures are lower than those e_0. The coefficient α in the equation (Fig. 3) defines how the hydraulic aperture decreases with increasing normal stress. For the fracture, we assigned half of the value used for the rock matrix. This enables the fracture aperture to decrease relatively slower with increasing normal stress based on an assumption that the pre-existing fractures have asperities which prevent the fracture surfaces from being completely closed, therefore the fluid flowing through the fractures is less influenced by the normal stress.

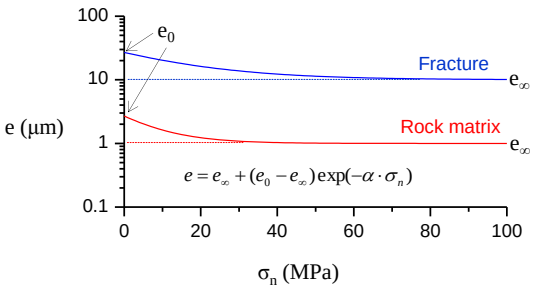

Fig. 3. Relations of hydraulic aperture (e) and normal stress (σ_n) applied to the intact rock and the fractures.

4. Simulation results

4.1. Influence of angle of approach on HF-NF interaction (Models 1 & 2)

Fig. 4 shows the distribution of fluid pressure and induced seismic events in Model 1 (Fig. 2a) and Model 2 (Fig. 2b). The results show that the orientation of the NFs with respect to the propagation direction of the HF has

a significant influence on the seismic event evolution. In Model 1 where the angle of approach of the HF to the NF is approximately 30°, the HF coalesces with the NF and the injected fluid migrates into the NF and progressively leads to shear failure of the NF as the fluid flows through the NF. This is the mechanism of "hydro-shearing". After the NFs are fluid filled, additional fluid injected then increases the level of stress concentration at the tips of the NFs. Further injection then leads to Mode I opening fractures at the tips of the NFs which propagate in wing-shape (Fig. 4c), identical to what is commonly observed in laboratory experiments of wing-fracture propagation at the tips of an inclined fracture by external loading [11, 12]. We refer to the wing-shape fracture propagation simulated in Model 1 as "hydro-wing" fracture. The hydro-wing fracture on the right tip of the right NF propagates without being driven by the fluid pressure as observed in the left hydro-wing fracture. This indicates that the right hydro-wing fracture in Mode I is not induced by the fluid pressure but rather triggered by the fluid pressure. Also comparing the seismic events that are placed along the traces of the NFs which are mostly in Mode II (Fig. 4e) with those of the hydro-wing fractures that are mostly in Mode I (Fig. 4e), it shows that the magnitudes of the seismic events along the hydro-wing fractures are slightly higher. This modeling result contradicts with what is commonly known, as Mode II shear failure tends to radiate larger seismic energy than Mode I tensile failure. Our results demonstrate that what is commonly known may not apply to hydraulically driven fracture propagation and interaction with natural fractures. In Model 2 where the angle of approach of the HF to the NF is approximately 60°, the HF reaches the NF but significantly less events are induced along the NF. The phenomenon observed in this model corresponds to HF arrest (Fig. 1a) and HF slippage and NF dilation (Fig. 1c).

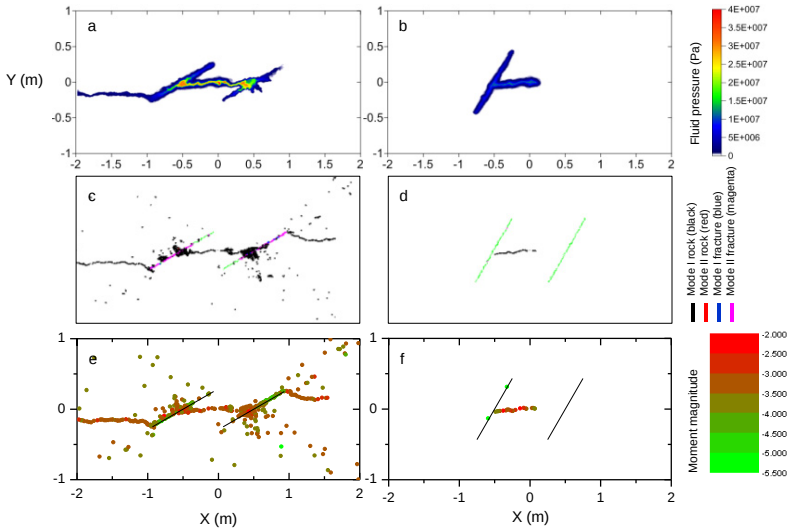

Fig. 4. Distribution of fluid pressure (a & b); cracks in PFC2D (c & d) and seismic events at the end of simulation of fluid injection with 30° inclined two NFs and 60° inclined two NFs. Seismic events are colored according to the moment magnitude provided by the color scale on the right.

4.2. Influence of fluid viscosity on HF-NF interaction (Model 3)

The two figures in the top row in Fig. 5 show the pressure distribution of fluid with a viscosity of (a) 1e-3 Pa·s and (b) 100e-3 Pa·s. The injection volume for both low and high viscosity cases is the same. In low viscosity model the injected fluid mostly flows into the NF, then leaks off into the rock matrix. The fracture propagation pattern becomes more complex at the region near the tips of the NFs. The two figures in the bottom row show the distributions of seismic events that are colored according to the magnitudes. Compared to the model with high viscosity fluid showing linear cluster pattern, the low viscosity fluid induces more events with volumetric cluster that are placed along the NFs, between the NFs, and beyond the tips of the NFs. At later stage of the simulation, more events are induced at the two far tips of the NFs and progress towards the model boundary and finally split

the model into two parts. The simulation results – volumetric fracture pattern by low viscosity fracturing fluid and linear fracture pattern by high viscosity fracturing fluid – are consistent with the experimental results by Ishida et al., where cubic granite specimens were hydraulically fractured by water and oil [13] and by supercritical and liquid CO_2 [14]. Their results showed the fracture patter induced by oil is planar with few branches, while water tends to generate thin and wavelike cracks with many secondary branches [13]. Acoustic emission distributions induced by supercritical CO_2 fracturing show larger fractal dimension (FD: 2.20 & 2.64) than those by liquid CO_2 fracturing (FD: 1.62 & 1.64) [14].

In the model with high viscosity fluid, the pattern of fracture propagation is less influenced by the NFs, and the seismic event clouds generated between the tips of the NFs are more linear with slightly lower magnitudes. In the model with low viscosity fluid, large number of seismic event is observed along the two outer NFs despite the fact that the injected fluid has less migrated into the NFs. Occurrence of those high magnitude events may have resulted from the "stress shadowing effect" [4, 15], where the fluid columns built up at two near NFs provides additional stress to the major principal stress locally at the area between the two tips of the NFs. The figure also shows that there are many seismic events located beyond the fluid column along the far left NF. These events are induced by a very small amount of fluid pressure perturbation. We refer to these events as "triggered events".

Similarity can be found in one example, although on a significantly larger scale, where massive wastewater injection in US Oklahoma has induced a sharp increase in seismicity since 2008 and led to several damaging earthquakes, i.e. M5.7 (moment magnitude) earthquake near Prague, Oklahoma [16]. A hydrogeological modelling study by Keranen et al. [17] suggested that the pore pressure change modelled at each hypocenter indicates a critical threshold of ~0.07 MPa, above which earthquakes are triggered, which is compatible with prior observations that static stress changes of as little as ~0.01 to 0.1 MPa are sufficient to trigger earthquakes when faults are near failure in the ambient stress field. In the modelling presented here, it is also observed that there are seismic events induced in the area with fluid pressure lower than 0.1 MPa, mostly along the trace of the NF of which the state of the stress became more near-critical by additional stress increase, i.e. stress shadowing effect, provided by the fluid columns in the NFs.

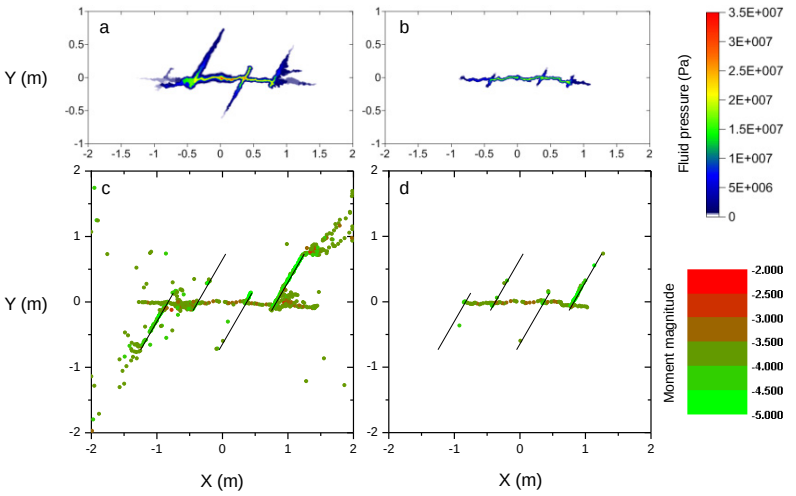

Fig. 5. Distribution of fluid pressure and seismic events at the end of simulation of fluid injection with viscosity of (a & c) 1e-3 Pa·s and (b & d) 100e-3 Pa·s. Seismic events are color coded according to the moment magnitude provided by the color scale on the right.

4.3. Evolution of seismicity in complex fracture networks (Model 4)

In this model, we investigate how the seismic events evolve in a complex network of fracture sets. Fig. 6 shows the distribution of (a) fluid pressure, (b) cracks (broken bonds), (c) seismic events color coded according to their moment magnitude and (d) stress drop. In the beginning, the HF created from the injection borehole propagates

horizontally in the direction of the major principal stress. After the HF meets the NF, the injected fluid migrates into the NF network and flows mainly through the NF network. Fluid pressure distribution shown in Fig. 6a demonstrates that the fluid is mostly flowing through the NF network and then slowly leaks off to the rock matrix. Fluid flowing through the NF network then lowers the normal stress and leads to failure of the smooth joints of the NFs in Mode II as shown in Fig. 6b and indicated in magenta. The mechanism involved here is "hydro-shearing".

After the NF network failed extensively in Mode II, the blocks of intact rock then fail due to shearing of the NFs in the network. Failure of the intact rock block in Mode I is shown in Fig. 6b. These failures in Mode I are then computed as seismic events with relatively large magnitude as shown in red in Fig. 6c. An observation is made in the spatial relation between the fluid pressure (Fig. 6a) and the distribution of cracks (Fig. 6b) and seismic events (Fig. 6c). The crack/event clouds extend more than the area where the fluid pressure is larger than 0.1 MPa. This indicates that the cracks/events occurring beyond the fluid pressure front (defined as 0.1 MPa fluid pressure) is triggered rather than being induced by the fluid injection. This phenomenon can be explained as follows. First, the injected fluid flows mainly into the NF network (Fig. 6a) and builds up fluid columns. The fluid columns then result in stress shadowing effects and slip of NFs. Slip of NFs results in increase in the normal stress on the NFs due to the dilation angle (Table 1). Therefore the state of stress on the NF increases and becomes more near-critical. At later times, fluid flows further through the NFs where the local stresses have increased and the NFs fail in Mode II, i.e. hydro-shearing. Due to the fact that the NFs fail under higher stress state, the amount of stress drop associated with hydro-shearing tends to be relatively large. Such large stress drop events are shown in Fig. 6d.

The observations made in this model may provide us with better understanding of how the fluid injection induced seismicity evolves in Enhanced Geothermal System (EGS) and how larger magnitude seismic events occur [18], e.g. Basel [19, 20], where the main mechanism for reservoir stimulation is hydro-shearing.

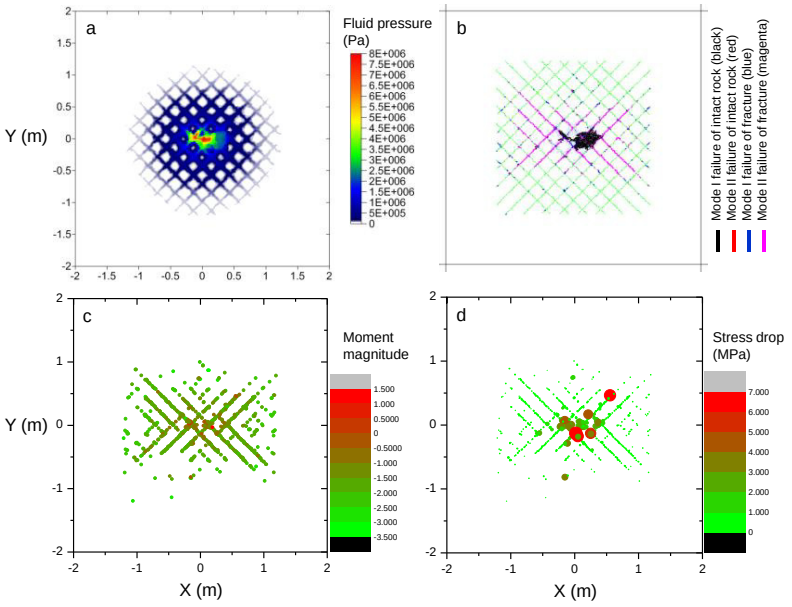

Fig. 6. Distribution of (a) fluid pressure; (b) cracks in PFC2D, seismic events colored according to the (c) magnitude; and (d) stress drop.

5. Summary

In this modelling study, we used the Particle Flow Code 2D (PFC2D) to simulate interaction of hydraulic fractures and natural fractures in low permeable hard rock. Natural fractures are simulated using the smooth joint model of PFC2D. The fluid flow algorithm that has been applied to several past modelling studies by Yoon et al.

was further developed by enabling the fracture network, represented by the smooth joint model, to behave differently from the rock matrix. This enabled the fracture network to have larger permeability. We performed a series of modelling cases to investigate possible interactions of hydraulic fractures and natural fractures by varying the angle of approach of the hydraulic fracture to the natural fractures and the fracturing fluid viscosity. The results demonstrate that the modelling tool is able to capture all possible interactions of hydraulic fracture and natural fractures that involve Arrest, Crossing, Slippage of hydraulic fracture, Dilation of natural fracture, Closing/Opening of natural fracture. Moreover, we used a seismicity computing algorithm to calculate the magnitude and seismic radiated energy from the simulated seismic events, which are the bond breaks. Simulations show that the hydraulic fracture propagating toward the natural fracture with low angle of approach coalesce and the fluid flows through the natural fractures and progressively results in hydro-shearing, and propagation of hydro-wing fractures at the tips that are mostly of Mode I type. With higher angle of approach, the hydraulic fracture is arrested by the natural fracture, and no fracture propagation further from the tips of the natural fractures were observed. We also tested the model containing multiple natural fractures with two different fluid viscosities. A hydraulic fracture generated by high viscosity fluid tends to be highly localized and less influenced by the natural fractures. However, hydraulic fractures generated by low viscosity fluid are highly influenced by the natural fracture network as fluid easily flows into it. Fluid-filled natural fractures then locally alter the stress field by stress shadowing which leads to a complex interaction between the natural fractures and the hydraulic fractures with relatively higher magnitude of induced seismic events. The evolution of seismic events in a complex network of natural fractures is simulated and the physical mechanisms involved in the development of relatively larger magnitude microseismic events are investigated. The simulation shows that the fluid flowing into and through the natural fracture network system results in an increase of local state of stress due to stress shadowing which is followed by hydro-shearing seismicity at a later stage. Applying the new fluid flow algorithm developed in this modelling study to a reservoir scale EGS is planned. We see the hydro-wing fracturing mechanism investigated in this study also as an efficient mechanism to operate in situ at reservoir scale for the permeability enhancement process in geothermal system.

References

[1] N. Zangeneh, E. Eberhardt, R.M. Bustin, Investigation of the influence of natural fractures and in situ stress on hydraulic fracture propagation using a distinct-element approach, Can. Geotech. J. 52 (2015) 926–946.

[2] Itasca Consulting Group Inc., Particle Flow Code in 2 Dimensions, Minneapolis, 2008.

[3] J.S. Yoon, A. Zang, O. Stephansson, Numerical investigation on optimized stimulation of intact and naturally fractured deep geothermal reservoirs using hydro-mechanical coupled discrete particles joints model, Geothermics 52 (2014) 165–184.

[4] J.S. Yoon, G. Zimmermann, A. Zang, Numerical investigation on stress shadowing in fluid injection-induced fracture propagation in naturally fractured geothermal reservoirs, Rock Mech. Rock Eng. 48 (2015) 1439–1454.

[5] J.S. Yoon, G. Zimmermann, A. Zang, Discrete element of cyclic rate fluid injection at multiple locations in naturally fractured reservoirs, Int. J. Rock Mech. & Min. Sci. 74 (2015) 15–23.

[6] J.S. Yoon, G. Zimmermann, A. Zang, O. Stephansson, Discrete element modeling of fluid injection-induced seismicity and activation of nearby fault, Can. Geotech. J. 52 (2015) 1457–1465.

[7] D. Mas Ivars, M.E. Pierce, G. Darcel, J. Reyes-Montes, D.O. Potyondy, R.P. Young, P.A. Cundall, The synthetic rock mass approach for jointed rock mass modelling, Int. J. Rock Mech. & Min. Sci. 48 (2011) 219-244.

[8] D. Chuprakov, O. Melchaeva, R. Prioul, Hydraulic fracture propagation across a weak discontinuity controlled by fluid injection, in: A.P. Bunger, J. McLennan, R. Jeffrey (Eds.), Effective and Sustainable Hydraulic Fracturing, InTech, Croatia, 2013, pp. 157–181.

[9] H. Hökmark, M. Lönnqvist, B. Fälth, THM-issues in repository rock Thermal, mechanical, thermo-mechanical and hydro-mechanical evolution of the rock at the Forsmark and Laxemar sites, Technical Report TR-10–23, SKB Swedish Nuclear Fuel and Waste Management Co., 2010.

[10] J.F. Hazzard, R.P. Young, Dynamic modelling of induced seismicity, Int. J. Rock Mech. & Min. Sci. 41 (2004) 1365-1376.

[11] B. Shen, O. Stephansson, H.H. Einstein, B. Ghahrcman, Coalescence of fractures under shear stresses in experiments, J. Geophys. Res. 100 (1995) 5975–5990.

[12] H. Lee, S. Jeon, An experimental and numerical study of fracture coalescence in pre-cracked specimens under uniaxial compression, Int. J. Solids Struct. 48 (2011) 979–999.

[13] T. Ishida, Q. Chen, Y. Mizuta, J.C. Roegiers, Influence of fluid viscosity on the hydraulic fracturing mechanism, J. Energy Resour. Technol. 126 (2004) 190–200.

[14] T. Ishida, K. Aoyagi, T. Niwa, Y. Chen, S. Murata, Q. Chen, Y. Nakayama, Acoustic emission monitoring of hydraulic fracturing laboratory experiment with supercritical and liquid CO2, Geophys. Res. Lett. 39 (2012) L16309.

[15] O. Kresse, X. Wend. H. Gu, R. Wu, Numerical modeling of hydraulic fractures interaction in complex naturally fractured formations, Rock Mech. Rock Eng. 46 (2013) 555–568.
[16] K.M. Keranen, H.M. Savage, G.A. Abers, E.S. Cochran, Potentially induced earthquakes in Oklahoma, USA: Links between wastewater injection and the 2011 M2 5.7 earthquake sequence, Geology 41 (2013) 699–702.
[17] K.M. Keranen, M. Weingarten, G.A. Abers, B.A. Bekins, S. Ge, Sharp increase in central Oklahoma seismicity since 2008 induced by massive wastewater injection, Science 345 (2014) 448–451.
[18] A. Zang, V. Oye, P. Jousset, N. Deichmann, R. Gritto, A. McGarr, E. Majer, D. Bruhn, Analysis of induced seismicity in geothermal reserovirs – An overview, Geothermics 52 (2014) 6–21.
[19] M.O. Häring, U. Schanz, F. Ladner, B.C. Dyer, Characterisation of the Basel 1 enhanced geothermal system, Geothermics 37 (2008) 469-495.
[20] Y. Mukuhira, H. Asanuma, H. Niitsuma, M.O. Häring, Characteristics of large-magnitude microseismic events recorded during and after stimulation of a geothermal reservoir at Basel, Switzerland, Geothermics 45 (2013) 1–17.